Analytic optical design of linear Fresnel collectors with variable widths and shifts of mirrors

R. Abbas*, J.M. Martínez-Val

Grupo de Investigaciones Termoenergéticas (GIT), Universidad Politécnica de Madrid, ETSI Industriales, José Gutierrez Abascal, 2, 28006, Madrid, Spain

A B S T R A C T

Linear Fresnel collectors still present a large margin to improve efficiency. Solar fields of this kind installed until current time, both prototypes and commercial plants, are designed with widths and shifts of mirrors that are constant across the solar field. However, the physical processes that limit the width of the mirrors depend on their relative locations to the receiver; the same applies to shading and blocking effects, that oblige to have a minimum shift between mirrors. In this work such phenomena are studied analytically in order to obtain a coherent design, able to improve the efficiency with no increase in cost. A ray tracing simulation along one year has been carried out for a given design, obtaining a moderate increase in radiation collecting efficiency in comparison to conventional designs. Moreover, this analytic theory can guide future designs aiming at fully optimizing linear Fresnel collectors' performance.

Keywords:
Linear Fresnel collector
Solar field layout
Optical efficiency
Monte Carlo Ray Tracing

1. Introduction

Linear Fresnel collector (LFC) technology seems to have a great potential to reduce the Levelized Cost of Energy (LCOE) in Concentrating Solar Power [1]. Even though the number of LFC plants in operation and construction is very low compared to parabolic troughs and central towers —see Fig. 1—, many scientific works have been published in the last years [2–19]. This is due to the fact that lineal Fresnel collectors have obvious economic advantages when compared to other technologies [1]:

- Only one receiver is used for the whole array of mirrors, and it is fixed. As a result, no rotating joints or flexible hoses are required, and therefore no environment or health issues due to hot oil leakages must be prevented. In addition, thanks to this configuration the tracked structure is lighter and thus the rotating mechanism is simpler.
- There is no need for glass-metal welds, which often cause receiver ruptures due to dilatation coefficient differences. Therefore the receiver is more robust.
- Mirrors are less expensive and easier to clean thanks to their low curvature. As the receiver does not move when the mirrors do, the latter may be rotated 180° for automated cleaning.

These capital and O&M cost advantages may drive to LCOE reductions of around 11% relative to parabolic troughs [22]. In addition, LFCs have many optic design variables, which include the width and position of each mirror. This could result in a better use of the reflective surface, as mirrors placed under the receiver may have different widths and different shifts [23,24] or gaps between two consecutive mirrors.

However, a design of the solar field with variable width and shift of mirrors across the field would require many design variables: each mirror would be defined by the transversal location of its central point x_i and its width W_i, assuming that the rotating axis of the mirror coincides with the centerline of the reflecting surface [14]. If the solar field has n mirrors, $2 \cdot n$ variables will be required to defined its geometry, in addition to the height of the receiver (assuming it is centered and horizontal).

Following Buckingham π theorem the geometrical configuration of the solar field may be expressed in terms of non-dimensional numbers. In this work such non-dimensionalization is carried out via the height of the receiver.[1] Therefore, in order to obtain the real value of any measurement in the transversal plane[2]

* Corresponding author. Tel.: +34 91 336 3023; fax: +34 91 336 3079.
E-mail addresses: rubenabbas@etsii.upm.es, ruben.abbas@upm.es (R. Abbas).

[1] The basic parameter for non-dimensionalization should be a variable that gives an idea of the lineal power of the plant. Therefore, either the height of the receiver or the total width of the field is recommended.

[2] The transversal plane is the plane perpendicular to the rotating axes of all mirrors; the field is defined in such plane, while the longitudinal axis (parallel to the rotating axes) is only important to obtain the distance traveled by the reflected beam.

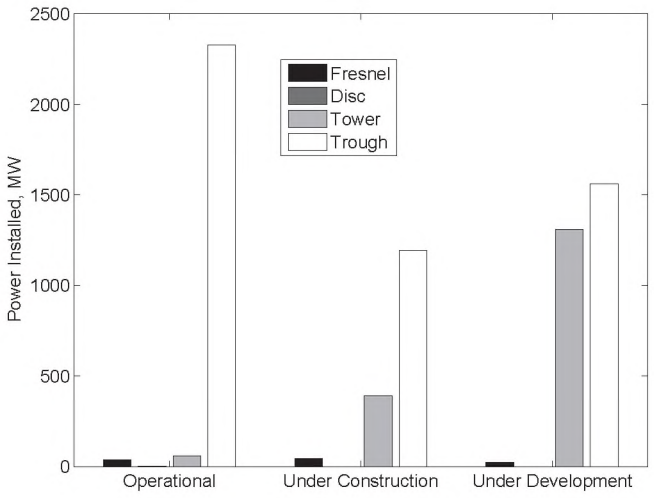

Fig. 1. Power (MW) of operational, in construction and in development CSP plants worldwide (data from Refs. [20] and [21], end 2012).

(width of mirrors, shift between mirrors, position, etc.), given values in this paper must be multiplied by the height of the receiver.

For the sake of an example, Fresdemo prototype (receiver height of 8 m) has 25 mirrors, while Puerto Errado (receiver height of 7.4 m) does 16 mirrors; this implies 50 and 32 variables to define the geometry of the solar field respectively, which would be hard to optimize numerically. From these variables, we can define the total width of reflecting surface, W_t, the width of the solar field, W_f, and the filling factor, FF:

$$W_t = \sum_{i=1}^{n} W_i \tag{1}$$

$$W_f = (x_n + W_n/2) - (x_1 - W_1/2) \tag{2}$$

$$FF = \frac{W_t}{W_f} \tag{3}$$

If all mirrors have the same width, W_i, and the shift between two consecutive mirrors, $x_{i+1}-x_i$, is constant, only three variables are necessary to define the geometrical configuration of the mirrors: the number of mirrors, n, their width, W_i, and the filling factor, FF, where the following formulas hold:

$$W_t = n \cdot W_i \tag{4}$$

$$W_f = W_t/FF \tag{5}$$

This solution has been adopted by multiple authors [25–28], and it is the option chosen for demonstration and commercial plants [29–31]. Obviously, the installation of mirrors with different widths would increase slightly the cost of the field due to economy of scales, but variable shift fields would not. Therefore, it seems that designs with variable widths and shifts of mirrors have not been considered for the sake of simplicity: the numerical optimization of the position and width of each mirror is time consuming, requiring genetic algorithms and very important computational resources. Nevertheless, the drawback to the simple design is that shading, blocking and deviations of reflected rays do not affect in the same way to mirrors centered in the field than to those in the lateral extremes.

Many works have been published addressing this problem. The first solution suggested was to install mirrors of the same width and shift by sections, so that different sections could have different filling factor depending on the distance to the centerline of the field [32]. This design concept would have as many variables as three times the number of sections, but it does not seem adequate to all mirrors.

Later, some authors identified a possible solution to LFC design consisting in, for a constant width of mirrors W_i across the field, shifting mirrors so that at noon there is no blocking. This was done assuming perfect tracking, although taking into account the reflected beam angle [3,4,24,33,34]. This has been done for different receiver shapes such as tubular, triangular, horizontally flat or vertically flat. In addition to such variable shift, some authors have included in their model variable width of mirrors across the field. Such studies suggest varying the width of mirrors so that the light reflected onto the receiver by each mirror has the same width, taking into account that the reflected beam at each point has a given aperture due both to the sun beam aperture and to reflecting errors [23,33,35,36]. This method would drive to a nearly constant concentration in the receiver if flat mirrors are used. Finally, some works have been published lately where the important matter in reflection is shading instead of blocking. In these papers, mirrors of the same width are placed in such way that, for a given sun elevation, no mirror is shadowed by its neighbor [11].

On the other hand, Chaves and Collares-Pereira [37] and Chaves and Collares-Pereira [38] try to minimize the blocking issue with a modified solution of the Compact Linear Fresnel Reflector presented by Mills and Morrison [39]: two receivers are used, one at each side of the field, so that mirrors may reflect the light towards one receiver or the other. In the Etendue-matched two-stage concentrator the height of mirrors is varied across the field, so that blocking effects are minimized even though the field has a very high filling factor.

This paper aims to give an analytical optical design in order to reduce coherently the number of design variables, so that the optimization of the width of mirrors across the field may be carried out. The study assumes the solar field to be installed in Planta Solar de Almería (PSA), with North-South orientation, where the receiver is located horizontally in the center of the field.

Section 2 describes the focusing procedure in LFC, as well as errors due to LFC design principle and to deviation of the solar beam from the reference position, which results in an optimum mirror width across the solar field. Section 3 explains the influence of the shift between two consecutive mirrors on shading and blocking effects, and finds a solution to this problem. An optical design model that considers both studies is presented in Section 4. Finally, conclusions and future works are discussed in last Section.

2. Optimum mirror width across the solar field

There are two sources of errors in the collection of energy: off-axis aberration, which causes a lateral drift of the reflected beam when the mirror is out of its reference position, and aperture of the reflected beam, caused by the geometries of the sun and the reflective surface. In this Section both sources and their consequence for different geometries are studied in order to optimize the width of the mirrors.

2.1. Variation of lateral drifts caused by off-axis aberration depending on design variables

Off-axis aberrations are a well known defocusing process that occurs in central tower solar fields. Linear Fresnel collectors also suffer this defocusing issue, due to the fact that the receiver is fixed

while the mirrors rotate to follow the sun. Thus, when a mirror is not in its reference position reflected beams do not impinge onto the receiver centerline.

However, the deviation of the reflected beam can be limited if the rotating axis coincides with an axis of the reflecting surface and the normal to the surface at such axis is at the bisector between the impinging sun beam and the line that links the axis with the receiver centerline. If this focusing procedure is followed then all reflected beams at a given physical point of the mirror are parallel to the reflected beam at such point at the reference position [14,40]. That is to say, the deviation of the reflected beam does not increase with the distance traveled after reflection, there is only a lateral drift of the reflected beam, which is parallel to the reference reflected beam.

Therefore, one may predict the maximum lateral drift analytically. Such maximum values depend on the actual reference position, which is defined as the position when the focus of the mirror is located in the central point of the receiver. There are two main reference positions [14]:

- Sun reference: All mirrors will be perfectly focusing at the receiver centerline when the sun is at its typical position. Such position is obtained via the weighted mean location of the sun in the transversal plane along the year. In a NS embodiment it coincides with the sun culmination at noon, which is the apparent zenith in the transversal plane; thus it is called zenithal reference. This reference drives to maximum concentrations at noon, but radiation may be more dispersed during the morning and evening.
- Specific reference: Each mirror will be perfectly focusing at the receiver centerline when the sun, the receiver central point and the mirror central point are aligned in the transversal plane. Doing so, only one mirror will be at its reference position at a time, thus maximum concentration will be slightly lower, but maintained more constant along the day.

Let us assume a field with North–South orientation, where a mirror of width W, designed with specific reference, is located such that the line that links it with the receiver makes an angle γ_R with the floor. If β is the angle made by the lines that link the center of the receiver with the center and with an extreme of the mirror, and α_{sr} and α_{ss} are the angles rotated by the mirror from the reference position at the effective sunrise and sunset times respectively, then the maximum lateral drift holds [14]:

$$d_{spe} = \frac{W}{2}\cdot\frac{1-\cos(\max(\alpha_{sr},\alpha_{ss})+\beta)}{\sin(\gamma_R-\beta)} \tag{6}$$

Equation (6) gives the maximum lateral drift in the reflection due to off-axis aberration when mirrors are designed with specific reference. If a zenithal reference embodiment is used the lateral drift is slightly smaller. Depending on whether the mirror rotates from the sun reference position to the apparent sunrise or sunset position (rotation of α_{sr} or α_{ss}), or towards the position where the mirror is perpendicular to the line that links it with the receiver (rotation of α_R), the off-axis aberration may occur in the internal side of the triangle made by the center of receiver and the extremes of the mirror ($d_{Zen\text{-}int}$) or in the external side ($d_{Zen\text{-}ext}$) respectively. A similar process such as the one followed by Abbas et al. [14] drives to the following Equations of the internal and external lateral drifts with sun reference:

$$d_{Zen-int} = \frac{W}{2}\cdot\frac{\cos(\alpha_R+\beta)-\cos(\alpha_{sr}+\beta)}{\sin(\gamma_R-\beta)} \tag{7}$$

$$d_{Zen-ext} = \frac{W}{2}\cdot\frac{1-\cos(\alpha_R+\beta)}{\sin(\gamma_R-\beta)} \tag{8}$$

In order to apply Equations (6)–(8) it is necessary to obtain the effective altitudes of the sun in the transversal plane at the sunrise and sunset. In order to establish these altitudes a new variable[3] is used: the ratio of sun radiation energy that is incident with an effective altitude smaller than the sunrise or sunset:

$$\begin{aligned} E_{sr<} &= \frac{\sum_{d=1}^{365} p_{sun}\int_{t=t_0}^{t_{sr}} \mathrm{DNI}\,dt}{\sum_{d=1}^{365} p_{sun}\int_{t=t_0}^{t_{end}} \mathrm{DNI}\,dt} \\ E_{ss<} &= \frac{\sum_{d=1}^{365} p_{sun}\int_{t=t_{ss}}^{t_{end}} \mathrm{DNI}\,dt}{\sum_{d=1}^{365} p_{sun}\int_{t=t_0}^{t_{end}} \mathrm{DNI}\,dt} \end{aligned} \tag{9}$$

where t_{sr} and t_{ss} are the times of each day when the impinging radiation has the direction of i_{sr} and i_{ss} respectively (choice in the design), t_0 is the first time of each day when $\mathrm{DNI} > \mathrm{DNI}_{min}$, t_{end} is the last time of the day when $\mathrm{DNI} > \mathrm{DNI}_{min}$ and p_{sun} is the clear-sky probability of each day.

Therefore, if a given value for $E_{sr<}$ and $E_{ss<}$ is chosen we can obtain the design altitude at the apparent sunrise and sunset, and thus maximum lateral drifts to be considered in the field. For example, an altitude at the apparent sunrise and sunset of 30° corresponds to a ratio of energy impinging with an angle below the design altitudes, $E_< = 0.11$. However, if the cosine factor is taken into account the actual energy impinging onto the mirrors is lower than 11%, as the impinging angle is very high when the sun altitude is so low.

The lateral drift across the field for different widths of mirrors is depicted in Fig. 2, where it has been assumed that the altitude of the sun at the effective sunrise is 30°. One may observe that the lateral drift increases both when the horizontal distance to the receiver and the width of the mirrors increase, as expected from previous equations. In addition, it appears that the value of the maximum drift for locations of the mirror far from the receiver is higher if a specific reference is considered than with zenithal reference. This is due to the fact that the maximum angle rotated from its reference is smaller for the latter, being constant across the field.

For the sake of an example, the Fresdemo prototype is 21 m wide, and so the distance from the furthest mirror to the receiver measured on the horizontal plane is 10.5 m, while the receiver height is 8 m; this implies a relative distance 1.31. On the other hand, all mirrors are 60 cm wide in such prototype, which gives a relative value of 0.075. Therefore, if the focusing procedure previously stated is perfectly followed, the maximum lateral drift will be somewhere around 0.03 in relative units in the case of specific reference, and bellow 0.025 for zenithal reference. This implies a drift around 20 cm in the Fresdemo, which is in agreement with the receiver installed in the prototype, that has a 50 cm wide secondary reflector. Therefore, if the reflected beam were collimated, all reflected radiation would impinge onto the receiver. Puerto Errado has been located in Fig. 2 as well, with a relative horizontal distance of 1.12, and a relative mirror width of 0.097.

[3] In North-South embodiment the design variable could have been the sun altitude at the apparent sunrise and sunset, which should be the same. However, in East-West configurations the minimum altitude of the sun at the North and at the South is different, so a variable to equilibrate losses at both sides is recommended.

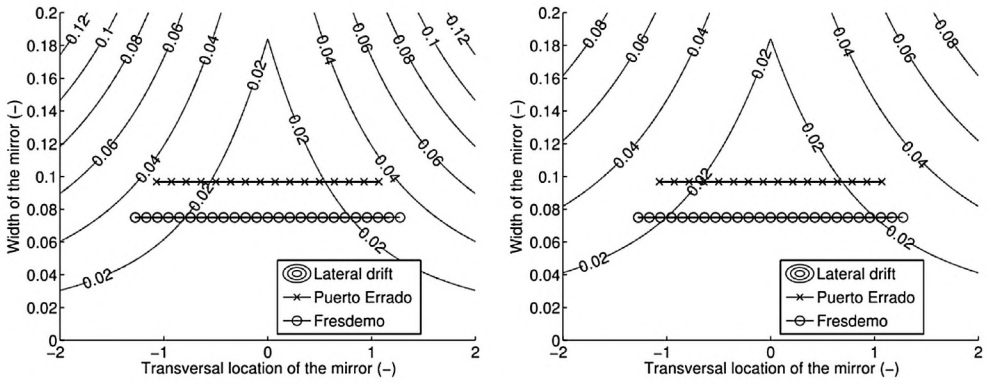

(a) Specific reference (b) Sun reference

Fig. 2. Maximum lateral drift depending on the horizontal distance from the mirror to the receiver and the width of the mirror, all in units relative to the receiver height for (a) specific reference and (b) zenithal or sun reference configurations.

2.2. Errors due to the sun shape and to the reflecting surface shape error

It is well known that impinging radiation from the sun is not collimated. The sun is seen from the Earth as a disc, with a radius that depends on the time of the year, the place where the solar field is located, and the atmospheric conditions [41]. However, we can consider in average that the impinging radiation in a point of the Earth has a direction within a cone with a half angle $\alpha_{pb} = 4.65$ mrad. The radiation probability density function within such cone may be modeled as a pillbox, although the actual flux probability density varies slightly from such pill-box [42–44].

Due to such variable impinging angle, reflected light would be spread within a cone with the same half angle even if reflection in the mirrors were perfect. Consequently, a beam reflected in a point of a mirror that impinges onto a receiver perpendicular to its direction would result in a circumference with a radius equal to the cone half angle times the distance traveled after reflection. However, it has been said that the receiver is assumed to be horizontal, and thus the shape of such reflected beam in a point of a mirror would be an ellipse. Therefore, the maximum transversal deviation in the receiver due to the shape of the sun is increased due the impinging angle.

In addition, the reflecting surface is never perfect, which enlarges the spreading effect. There are three sources of errors in the reflection [45]:

- Slope errors: the slope of the reflecting surface has macroscopic and medium scale errors, with a standard deviation of the tilt σ_S
- Reflectance errors: the microscopic topography of the reflecting surface gives an extra uncertainty in the reflected ray with a standard deviation of σ_R
- Tracking errors: the tracking system introduce an extra uncertainty in the tilt of the reflecting surface at each point with a standard deviation σ_T

If all sources of errors are considered to have circular Gaussian distribution, global errors in the reflected beam may be considered to have the same distribution with an effective dispersion that holds [45–48]:

$$\sigma_{ef}^2 = \sigma_R^2 + (2\sigma_S)^2 + (2\sigma_T)^2 \tag{10}$$

where the factor 2 that multiplies σ_R and σ_T is due to the fact that an error of x mrad in the tilt of the reflecting surface implies a deviation of the reflected beam of $2x$ mrad. The value of σ_{ef} at the state of the art is around 5 mrad [45].

It has been assumed that errors due to the sun shape follow a pill-box distribution, while the reflecting surfaces errors are Gaussian. In order to make an analytical study such distributions must be made equivalent. The mean square width, $\langle\rho_{pb}^2\rangle$ for a pill-box distribution depends on the half-angle of the impinging beam, α_{pb}. Such mean square width can be made equivalent to the mean square width of a pill-box distribution $\langle\rho_G^2\rangle$. Both values hold [48,49]:

$$\begin{aligned}\langle\rho_{pb}^2\rangle &= \frac{\alpha_{pb}^2}{2}\\ \langle\rho_G^2\rangle &= 2\cdot\sigma_G^2\end{aligned} \tag{11}$$

Therefore, the dispersion of the equivalent Gaussian distributions for a pill-box results:

$$\sigma_{pb}^2 \approx \left(\frac{\alpha_{pb}}{2}\right)^2 \tag{12}$$

If individual scattering distributions are normal, their convolution is also a normal distribution whose dispersion, σ_{tot}, is given by the square root of the sum of the squares of the individual dispersions [48,50]. Thus, the total dispersion, σ_{tot}, mean square width, $\langle\rho_{tot}\rangle$, a half-angle of the equivalent pill-box distribution, α_{tot}, can be obtained:

$$\begin{aligned}\sigma_{tot} &= \sqrt{\sigma_{pb}^2 + \sigma_G^2} = 5.51 \text{ mrad}\\ \langle\rho_{tot}\rangle &= \sqrt{2\cdot\sigma_{tot}^2} = 7.80 \text{ mrad}\\ \alpha_{tot} &= \sqrt{2\cdot\langle\rho_{tot}^2\rangle} = 11.03 \text{ mrad}\end{aligned} \tag{13}$$

The result of this approximation is observed in Fig. 3. This Figure depicts the probability of a reflected ray to be within a cone of a given half angle (*Any direction*), or within two longitudinal planes that form a given half angle (*Transversal direction*). This is done for the exact model –where the sun intensity distribution is assumed to follow Buie model [42–44]and the reflective surface shape to give an extra error with 5 mrad Gaussian distribution– and for the approximated model –where reflected rays are assumed to have an angle with normal direction which follows a Gaussian density probability whose dispersion is 5.51 mrad. One may observe that both models drive to similar solutions, and

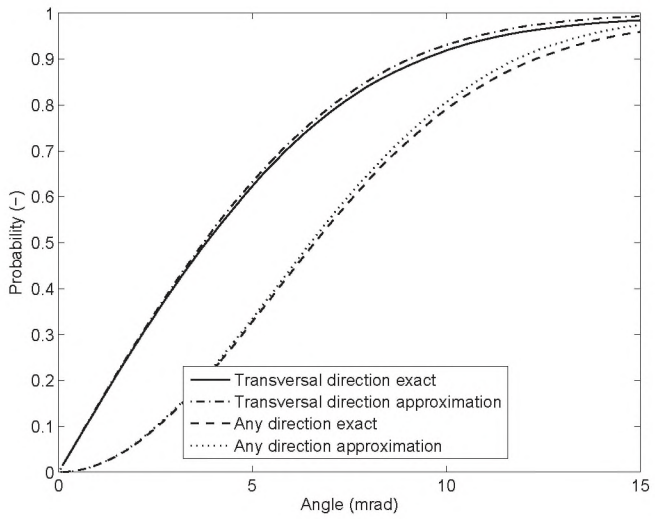

Fig. 3. Probability of a reflected ray to be within a cone of a given half angle (Any direction), or within two longitudinal planes that form a given half angle (Transversal direction), for an exact model versus a Gaussian approximation.

therefore it is a good option to assume the mean square width of reflected errors to be 7.8 mrad.

Linear Fresnel collectors being linear concentrators, the value that must be taken into account is the ratio of energy collected in the transversal direction. After Fig. 3 this ratio would be around 83% if the half angle is 7.8 mrad, and around 95% if the half angle considered is 11.03 mrad. This range of values seems adequate, as including a higher ratio of rays would imply very large half angles.

Finally, the distance traveled by the reflected ray must be calculated. Such distance measured in the projection plane only depends on the solar field configuration, as it is given by the receiver height and the horizontal distance from the mirror to such receiver. The distance traveled by the reflected beam in the transversal plane is $\sqrt{1+x^2}$, where x is the transversal location of the mirror respect to the receiver. However, the reflected ray also has a longitudinal component, which increases the distance traveled. Such component will be very important in winter for N–S configuration, and nearly negligible in summer [17].

The effective distance traveled by the reflected ray may be obtained by a weighted mean value of the distance via the energy impinging onto the mirror at each instant. Such weighted mean value results in a distance 15.6% higher than the distance measured in the transversal plane for the case of Almería. Therefore, the increase factor in this work gets a value $k = 1.156$, which covers half of the year in Spain. As a result, the transversal error of the reflected ray in a horizontal receiver due to the shape of the sun and the reflective surface holds:

$$r_{\text{cone}} = \frac{\langle \rho_{\text{tot}} \rangle k \sqrt{1+x^2}}{\sin(\gamma_R - \beta)} \tag{14}$$

2.3. Optimum width of the mirrors

It has been said that errors due to mirror defocusing and those given by the sun and reflecting surface shapes depend differently on the distance from the mirror to the receiver. As both sources of errors are proportional to $1/\sin(\gamma_R - \beta)$, there is no need to take this factor into account to compare them. This is equivalent to assume that the receiver is perpendicular to the reflected beam for each mirror.

Fig. 4 depicts maximum errors due to lateral drift, both for specific and zenithal reference, and due to the sun and reflective surface shapes. It is assumed that the relative width of all mirrors is 0.075, as it is in the Fresdemo, that the sun altitude at the effective sunrise is 30°, i.e. $E_>$ 0.11, and that the half width of the reflected beam that must be collected is 7.8 mrad — therefore some losses are assumed.

One can observe that, for those mirrors close to the receiver, errors due to the shapes of sun and mirror increase very slowly while those due to lateral drifts have their maximum rate of increase. The first fact is due to the small value of x, negligible compared to the height of the receiver. On the other hand, in these locations the variation of the transversal position has a deeper impact on the angle rotated by the mirror. However, when mirrors are placed further from the receiver, the maximum angle rotated by the mirror tends asymptotically to a maximum value, variations being smaller, while the horizontal distance traveled by the reflected ray becomes more important in respect to the receiver height. As a result, errors caused by the sun and mirror shapes become more important for the furthest mirrors.

This has an important influence on the adequate solar field design. There must be coherence in the mirrors width choice: it is worthless to install very narrow mirrors when there is an important error due to the distance traveled by the ray. Therefore, it seems interesting to vary the mirrors width across the solar field in such a way that the errors due to lateral drift have similar consequences as those caused by the sun and mirror surface shapes.

Fig. 5 shows the optimum mirror width after this principle depending on the horizontal distance to the receiver both for specific and sun reference embodiments. For central mirrors, as they get further from the receiver, their optimum width decreases due to the fact explained in previous paragraphs. A minimum optimum width is obtained approximately when horizontal distances from the receiver are slightly below the height of the receiver. When mirrors get even further from the receiver the error due to the distance traveled become too important and thus there is no point in continue reducing the width of the mirror.

For the sake of an example, the widths and transversal location of all mirrors in Fresdemo and Puerto Errado solar fields are also depicted in Fig. 5. One may observe that their widths are in the same order of magnitude of calculated optimum widths, which strengths this model.

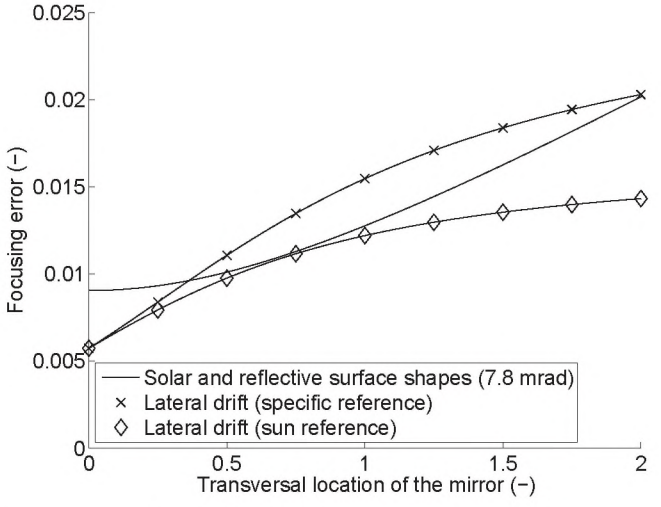

Fig. 4. Errors, in a receiver perpendicular to the reflective beam, due to lateral drift and sun and reflective surface shapes, for a fixed mirror width of 0.075 in relative units.

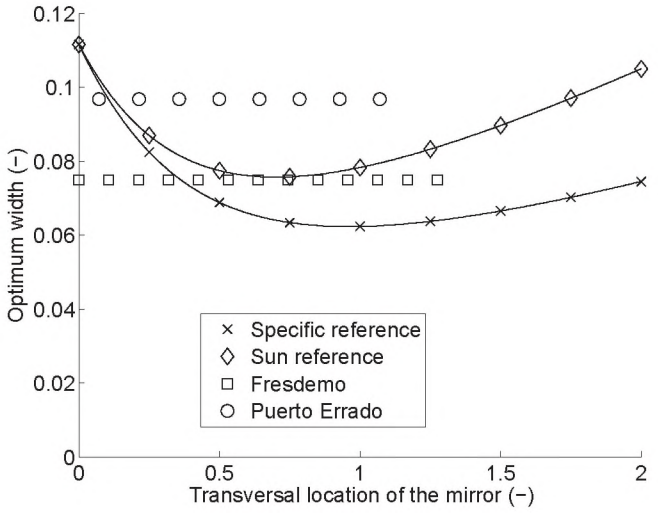

Fig. 5. Optimum width of the mirrors depending on the horizontal distance to the receiver for specific and zenithal (sun) references, assuming the accepted cone half angle to be 7.8 mrad and the sun altitude at the effective sunrise and sunset to be 30°. Widths of mirrors in Fresdemo and Puerto Errado solar fields are also depicted.

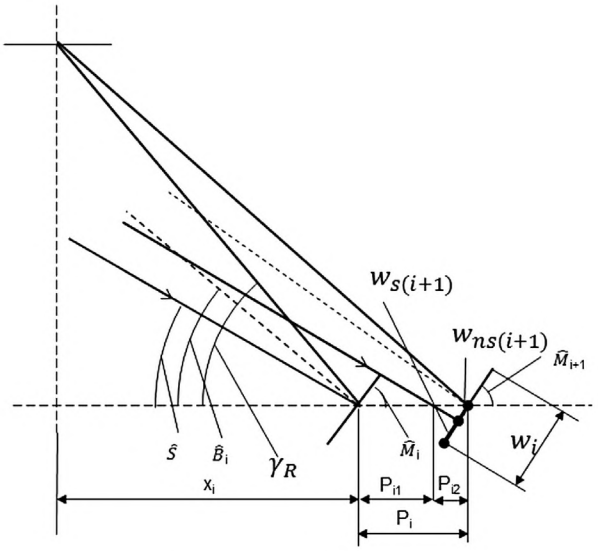

Fig. 6. Shading process in a pair of consecutive mirrors.

Finally, one may observed that the optimum width for a given location is wider if a zenithal reference configuration is chosen. This is thanks to the lower lateral drifts that appear with such configuration, as the angle rotated by the mirror from the reference position, both to the sunrise position and to the position where the mirror is perpendicular to the line that links it to the receiver, is limited, see Equations (6)–(8). Therefore, a zenithal reference has an advantage in respect to specific reference, because less mirrors are required for a given total reflecting width across the field.

3. Optimum shift between two consecutive mirrors across the solar field

Shading and blocking effects depend on the location of a given mirror and its distance to the neighboring mirrors, as well as on the effective sunrise and sunset altitude angles. Therefore, in order to equilibrate such losses across the field, the shift between two consecutive mirrors should vary as the distance to the receiver increases for a given effective sunrise angle. In this Section an analytical study is carried out to determine the optimum shift between mirrors.

A mirror in an LFC array is characterized by its rotation axis location, x_i, which coincides with the central point of the mirror. The height of the receiver being fixed (one relative unit), such location conveys a fixed angle γ_R between the transversal axis (where the central points of all mirrors are located) and the straight line going from the rotation axis to the receiver centerline. The mirror has a given width w_i, and at a given time of the day the mirror is tilted an angle $\widehat{M}_i$ with the transversal axis in order to focus the reflected solar ray from its central point onto the receiver centerline. Its neighboring mirror to the right will be located at x_{i+1}, with a shift between them $P_i = x_{i+1} - x_i$. Defined variables may be observed in Fig. 6.

Following the focusing criterion defined in Refs. [14,40], the normal to the mirror at its rotating axis coincides with the bisector between the impinging beam and the line that links the mirror and the receiver in the transversal plane. Such normal makes an angle $\widehat{B}_i$ that depends on the solar rays angle $\widehat{S}$, which also affects the tilt $\widehat{M}_i$:

$$\widehat{B}_i = \frac{\gamma_R + \widehat{S}}{2} \tag{15}$$

$$\widehat{M}_i = \pi/2 - \widehat{B}_i \tag{16}$$

The shading losses factor, f_s, is defined as the ratio of the surface of a given mirror under the shadow of the neighboring mirror. Applying the sinus theorem to the triangles that appear in Fig. 6 it results:

$$\frac{P_{i1}}{\sin\left(\pi - \widehat{S} - \widehat{M}_i\right)} = \frac{w_i/2}{\sin\left(\widehat{S}\right)} \tag{17}$$

$$\frac{w_{ns(i+1)}}{\sin\left(\widehat{S}\right)} = \frac{P_{i2}}{\sin\left(\pi - \widehat{S} - \widehat{M}_{i+1}\right)} \tag{18}$$

If we take into account that $P_i = P_{i1} + P_{i2}$, it results from previous equations:

$$w_{ns(i+1)} = \min\left(\left(P_i - \frac{w_i}{2}\frac{\sin\left(\pi - \widehat{S} - \widehat{M}_i\right)}{\sin\left(\widehat{S}\right)}\right) \times \frac{\sin\left(\widehat{S}\right)}{\sin\left(\pi - \widehat{S} - \widehat{M}_{i+1}\right)}, \frac{w_{i+1}}{2}\right) \tag{19}$$

which is negative if the area of the mirror $i+1$ under the shadow is beyond its central point. Therefore, the shading losses factor of mirrors $i+1$ at a given time holds:

$$f_{s(i+1)} = \frac{\frac{w_{i+1}}{2} - w_{ns(i+1)}}{w_{i+1}} \tag{20}$$

One can observe that the only design variables that affect the shading factor for a given sun altitude, $\widehat{S}$, are the distance between two neighboring mirrors, P_i, and mirror widths, w_i and w_{i+1}. Apparently the shading factor also depends on the tilts of the mirrors, $\widehat{M}_i$ and $\widehat{M}_{i+1}$, but they are function of angles $\widehat{S}$, γ_{Ri} and γ_{Ri+1}, see Equations (15) and (16), and thus they are given by the location of the mirrors and the time of the day.

For each sun position, $\widehat{S}$, shading will be maximized in mirrors where $(\pi - \widehat{S} - \widehat{M}_i) \approx \pi/2$ and $(\pi - \widehat{S} - \widehat{M}_{i+1}) \approx \pi/2$, i.e. when the mirrors, the receiver and the sun are approximately in the same line, which is the specific reference position. Obviously, shading will be more important when the sun altitude in the transversal plane is lower: during the early hours in the morning and late in the afternoon for NS solar fields, and during winter if it is oriented EW. This fact has a higher impact than the exact location of the mirror.

In addition to the shadows between mirrors, it may happen that a ray that is reflected in a given mirror is intercepted by the neighboring mirror on its path to the receiver; this process is called blocking. A similar analytical study has been carried out in order to determine the blocking effect factor along the day for each solar field configuration. First, the width of the half mirror that is not blocked, $w_{\mathrm{nb}(i+1)}$, is obtained:

$$w_{\mathrm{nb}(i+1)} = \min\left(\left(P_i - \frac{w_i}{2}\frac{\sin\left(\pi - \gamma_{Ri+1} - \widehat{M}_i\right)}{\sin(\gamma_{Ri+1})}\right) \times \frac{\sin(\gamma_{Ri+1})}{\sin\left(\pi - \gamma_{Ri+1} - \widehat{M}_{i+1}\right)}, \frac{w_{i+1}}{2}\right) \tag{21}$$

Low values of γ_R will minimize, or even make negative, the area of the lower half of the mirror with no blocking. Therefore, blocking processes are more important in mirrors far from the receiver. In addition, for a given position blocking effects are maximized when $(\pi - \gamma_{Ri+1} - \widehat{M}_i) \approx \pi/2$, i.e. when mirror x_i is perpendicular to the straight line that links mirror x_{i+1} rotation axis with the receiver. This happens approximately when the sun, the receiver and the mirror are aligned in the transversal plane.

Once $w_{\mathrm{nb}(i+1)}$ is obtained, the blocking losses factor can be defined as:

$$f_{\mathrm{b}(i+1)} = \frac{\frac{w_{i+1}}{2} - w_{\mathrm{nb}(i+1)}}{w_{i+1}} \tag{22}$$

The present analytical study has driven to a model in order to depict the consequences of shading (left) and blocking (right) along a given day, see Fig. 7. The Fresdemo configuration has been chosen again in terms of the shift between mirrors and their widths.

One can observe that, as it would be expected, shading has a higher impact when the sun is low – the solar angle $\widehat{S}$ varies in the range of 20°–160° in this simulation. During the morning, mirrors placed in the Western side suffer more shading effects, while in the afternoon those in the Eastern extreme do. Actually, at each time of the day the maximum shading effect would occur for mirrors in the specific reference position, i.e. when the impinging sun is perpendicular to the mirror surface, but when the sun is high enough such effects do not exist.

When comparing blocking (Fig. 7-right) to shading (Fig. 7-left) one may observe that the former implies lower effects than the latter, maximum values being around 12% for the Fresdemo field configuration. However, mirrors located in the extremes of the mirrors array suffer blocking processes during a longer period of the day, the effect not being negligible. On the other hand, while shading effects appear in all mirrors across the solar field along the day, blocking effects only affect to those mirrors far away from the receiver.

When one mirror suffers shading and blocking at the same time, both terms affect to the lower part of the mirror; therefore only the effect that has a higher factor should be considered in a global study. As a result, one can define the total losses factor for each mirror at each given time as follows:

$$f_{\mathrm{t}} = \max(f_{\mathrm{s}}, f_{\mathrm{b}}) \tag{23}$$

Thus, comparing Fig. 7 left and right, blocking effects would only be important after 10:30 in the morning and before 18:00 in the afternoon. However, if the solar field is wider the effect of blocking would appear at an earlier time in the morning and later in the afternoon.

When optimizing the solar field, the design may look for a mirror distribution where the mean total losses factor, $\overline{f_{\mathrm{t}}}$, is the same for all mirrors. Such average is defined, for each mirror, as follows:

$$\overline{f_{\mathrm{t}}} = \frac{\sum_{d=1}^{365}\int_{t_0}^{t_{\mathrm{end}}} f_{\mathrm{t}}(t)\mathrm{d}t}{\sum_{d=1}^{365} t_{\mathrm{end}} - t_0} \tag{24}$$

Alternatively, this average could be weighted with the Direct Normal Irradiance (DNI) at each time of the day and of the year obtaining the energy total losses factor, $\overline{f}_{t_{\mathrm{E}}}$. Such factor would give the energy lost by the mirror due to shading or blocking effect, and it takes into account the clear sky factor for each day (Almería).

$$\overline{f}_{t_{\mathrm{E}}} = \frac{\sum_{d=1}^{365}\int_{t_0}^{t_{\mathrm{end}}} f_{\mathrm{t}}(t)p_{\mathrm{sun}}\mathrm{DNI}(t)\mathrm{d}t}{\sum_{d=1}^{365}\int_{t_0}^{t_{\mathrm{end}}} p_{\mathrm{sun}}\mathrm{DNI}(t)\mathrm{d}t} \tag{25}$$

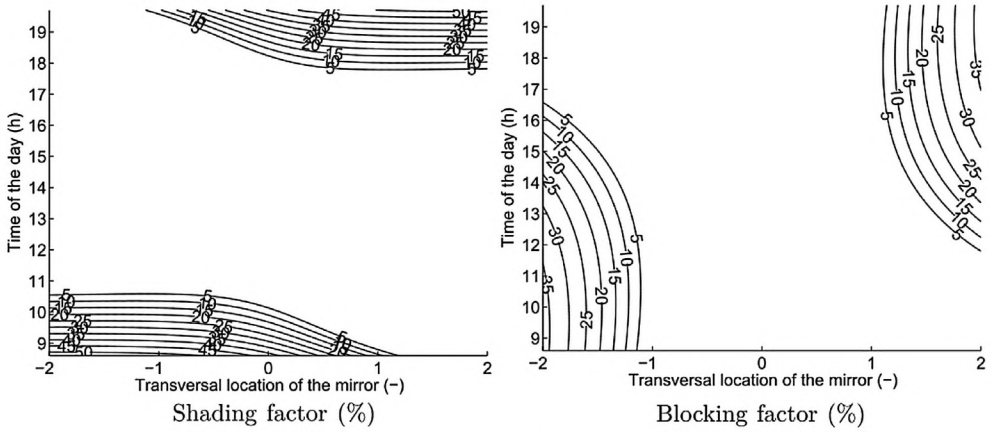

Fig. 7. Shading (left) and blocking (right) losses factors (% of the impinging radiation) in the Fresdemo solar field along the day 21st June, as a function of the time (y axis) and the location of the mirror in the solar field x axis (also graph x axis).

However, the energy impinging onto each mirror per unit width is not the same across the solar field. Mirrors located in the central part of the field reflect more energy along the day due to the fact that the maximum angle made by the normal to the mirror with the incident beam is limited. Therefore, another mean factor appears: the specific energy total losses factor, $\overline{f}_{t_e}$. Such factor is defined as the average energy losses due to shading and blocking per unit width of the mirror divided by the average impinging energy onto the mirrors of the field per unit width of mirrors:

$$\overline{f}_{t_e} = \frac{\sum_{d=1}^{365} \int_{t_0}^{t_{end}} f_t(t) p_{sun} \mathrm{DNI}(t) \mathrm{d}t}{\sum_{d=1}^{365} \frac{\sum_{i-1}^{n} \int_{t_0}^{t_{end}} W_i p_{sun} \mathrm{DNI}(t) \mathrm{d}t}{\sum_{i-1}^{n} W_i}} \tag{26}$$

Such losses factors, mean, energy and specific energy, are depicted in Fig. 8 in terms of shading, blocking and total effects for the case of the Fresdemo prototype.

One can observe that, in the case of central mirrors, the only process that has an influence on the mean total factor is shading (see Fig. 8a). Furthermore, even though the maximum value of shading factor appears in the lateral mirrors, central mirrors are affected by a higher average value due to the longer period of the day -morning and afternoon-when mirrors are partially under the shadow of the neighboring mirrors.

On the other hand, lateral mirrors are affected by both shading and blocking effects. Despite the blocking losses factor having a lower mean value along the day than the shading losses factor, it has been observed that they do no happen always at the same time. Therefore both processes contribute to diminish the performance of the mirror. As a result, the mean total losses factor is larger for the lateral mirrors than for the central ones. This difference would have been even larger if the solar field were larger.

If we consider the actual energy that impinges onto each mirror (Fig. 8b), shading losses factors in central mirrors decrease due to the fact that when the sun intensity is higher there are no shadows in such mirrors. This is not seen that clearly in lateral mirrors, as in that case shading effects occur until later in the morning, or from earlier in the afternoon.

Finally, one may observe in Fig. 8c that if we take into account the average loss per unit of width of mirrors, the value increases slightly in the central part of the field, where the impinging solar energy is higher. This factor may be considered as the most interesting one to equalize across the field: a square meter of reflecting surface has the same price, no matter where it is placed, and thus losses (part of the mirror that is not used) should be the same.

From these Figures it results that the shift between any two consecutive mirrors of the solar field should not be the same. Instead, it should be chosen so that the specific energy total losses factor is the same for all mirrors. Doing so, the use of the all the reflecting surface would be more coherent. In Fig. 8c the change in this factor is not very important for central mirrors, but it is when blocking processes take place. In addition, the fact that $\overline{f}_{t_e}$ does not vary importantly is due to the configuration of the Fresdemo, where the filling factor is 71.4% and the width of mirrors is constant. If these constrains are changed, as suggested in Section 2, the shift between mirrors will need to vary across the field in order to make the specific energy total losses factor constant.

4. Results: an improved optical design for LFC

The final goal of this paper is to obtain an analytical optical design of the solar field where the design variables are only three, as it happens in a solar field where all the mirrors have the same

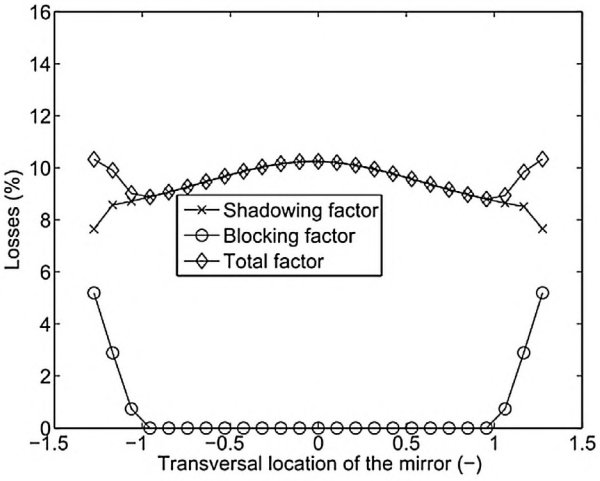

(a) Mean factors

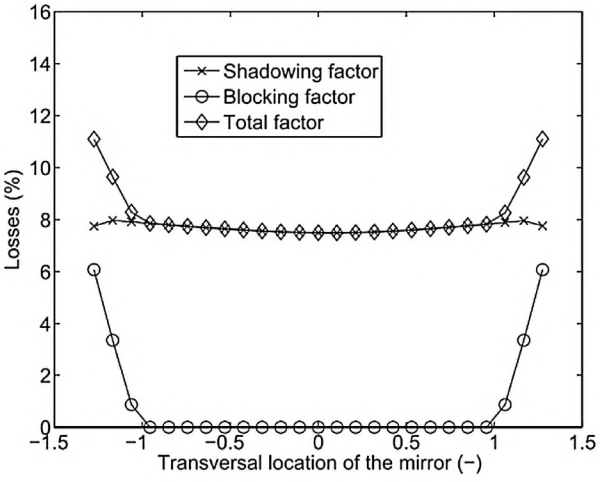

(b) Energy factors

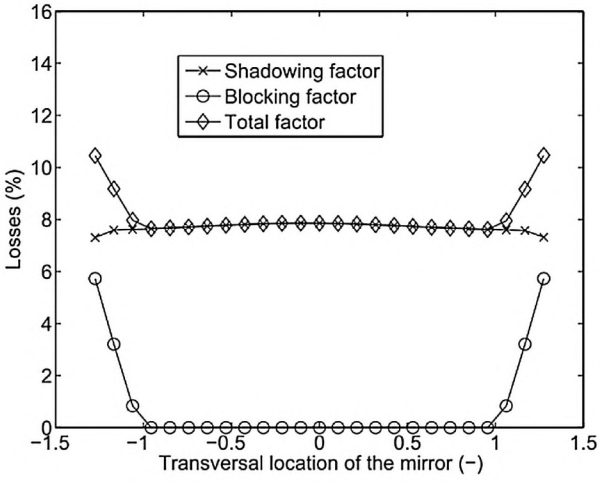

(c) Specific energy factors

Fig. 8. Mean (a), energy (b) and specific energy (c) losses factors (%), for shading, blocking and total effects, in the Fresdemo solar field depending on the location of the mirror in the solar field x axis.

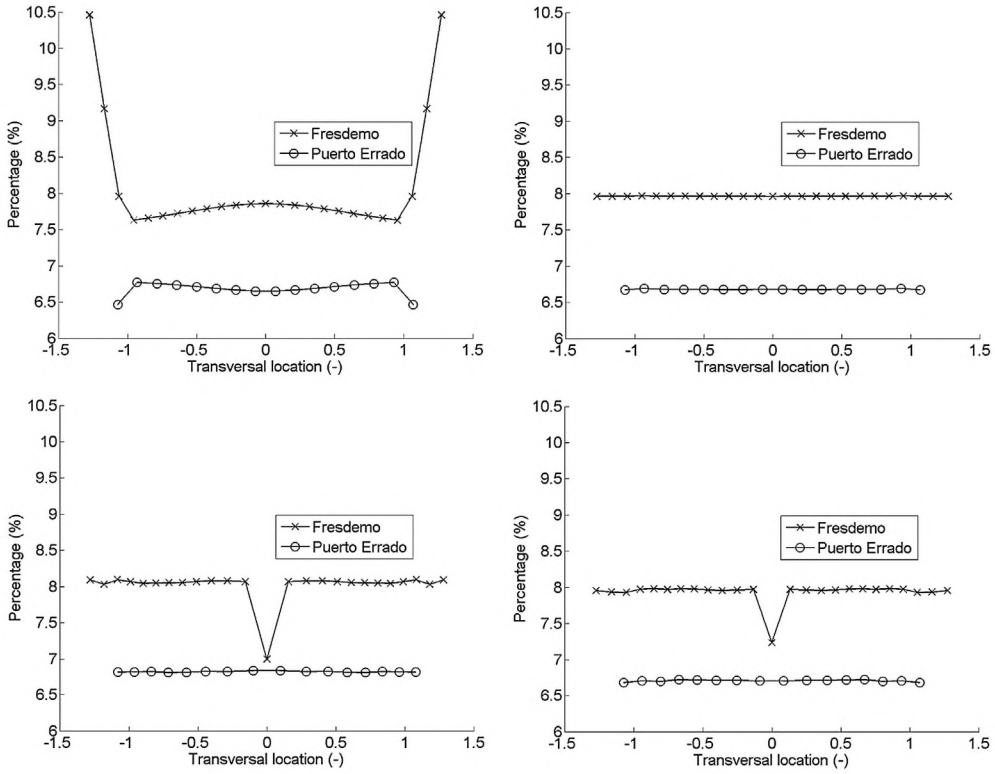

Fig. 9. Specific energy losses factors with Fresdemo and Puerto Errado design variables for constant width and shift (upper left), constant width and variable shift (upper right), and variable shift and width with specific reference (lower left) and sun reference (lower right).

width and shift. Such variables would be the number of mirrors, the solar field width (compared to the height of the receiver) and the filling factor.

The width of each mirror depending on its transversal location will follow *a priori* Fig. 5, depending on whether the reference adopted for the mirror curvature is zenithal or specific. Then, the shift between mirrors is varied so that all mirrors[4] have the same specific energy losses along the year, i.e. they have the same specific energy total losses factor $\overline{f}_{t_e}$.

In Section 2 the ratio of energy impinging when the sun altitude is bellow a given angle, $E_<$, has been introduced. Such ratio may be considered as a design variable, which drives to the sun altitude at the effective sunrise and sunset. If there is a need to increase the mean width of mirrors the designer should increase the value of the variable $E_<$. In addition, the choice of $\overline{f}_{t_e}$, together with $E_<$, determines the mean shift between two consecutive mirrors, and thus the filling factor. Thus, this new design of LFCs consists in finding the values of $E_<$ and $\overline{f}_{t_e}$ that drive to the desired field width and filling factor for the number of mirrors adopted.

Such variable width and shift design may carry an extra cost: the width of pair of mirrors (at both sides of the receiver) varies across the field, which may increase manufacturing costs. There is an intermediate solution between the variable width and shift design and the homogeneous design: constant width and variable shift. This alternative design would drive to a solar field where losses due to shadowing and blocking are equilibrated, although the width of mirrors is constant and equal to the homogeneous design (given by Equation (4)).

For the sake of an example, designs with constant width and variable shift and with variable width and shift of mirrors have been developed using the design variables —number of mirrors, total width and filling factor— of Fresdemo and Puerto Errado. Fig. 9 depicts the specific energy total losses factors for all mirrors with such configurations.

One may observe that for all new designs, the specific energy total losses factor maintains approximately constant for each design (with maximum differences of 0.5% related to its mean value). In the case of Fresdemo design variables, the value is in all cases a little higher than for the central mirrors of the homogeneous design, in order to reduce blocking effects in the lateral mirrors. On the other hand, in the case of Puerto Errado new design factors are smaller for central mirrors than in the constant width and shift design.

As previously predicted, if the number of mirrors is odd it is not possible to make all mirrors have the same specific energy losses due to the fact that the central mirror is wider and its position is fixed. This is not the case of even number of mirrors, where we can vary the distance between the two central mirrors in order to adjust their losses. We can also observe that the specific energy factor increases with the filling factor: Fresdemo and Puerto Errado have filling factor of 71.43% and 69.23%. However, this relation between filling factor and specific energy factor is not lineal.

It has been observed that the specific energy losses factors due to shading and blocking are reduced with this variable width and shift design. Nevertheless, the reduction in such losses does not necessarily imply that the efficiency of the new system is better: increase of lateral drifts due to the larger widths of central mirrors may drive to a higher dispersion if the reduction in the extreme mirrors size does not have a higher impact.

[4] If there is an odd number of mirrors it is not possible to make the central mirror have the same specific energy losses as other mirrors. This is due to the fact that its position is constrained ($x = 0$) and its width is higher than the width of mirrors around; thus, specific energy losses in the central mirror will always be lower.

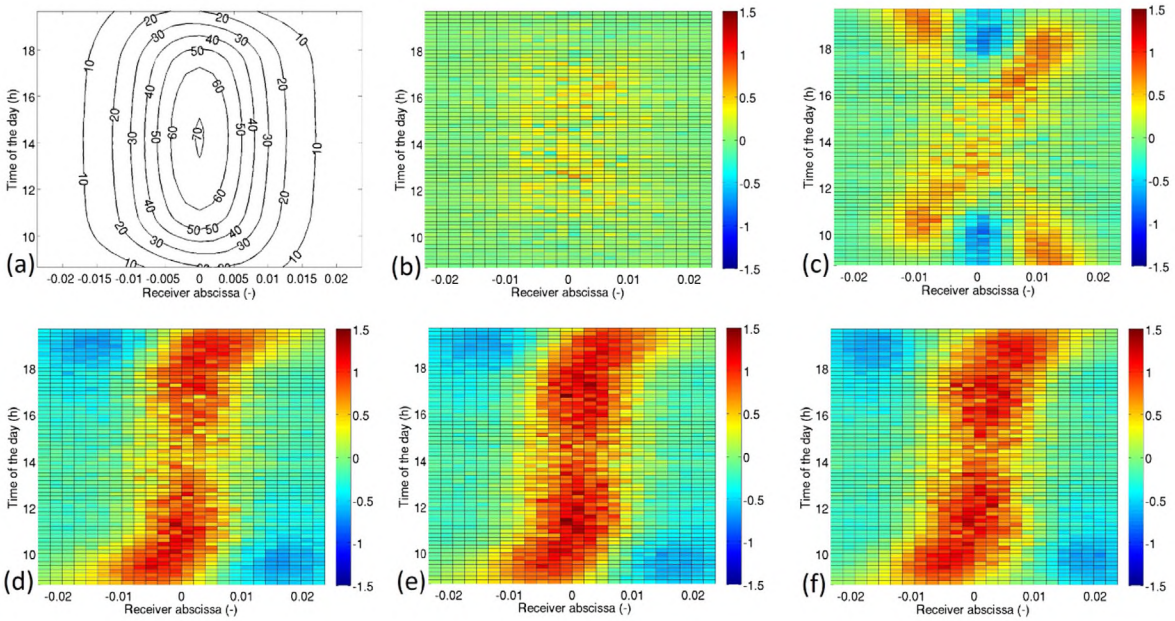

Fig. 10. Radiation flux (kW/m^2) across the receiver for a Fresnel solar field with Fresdemo design variables with constant width and constant shift of mirrors with specific reference (a), and difference in radiation flux (kW/m^2) across the receiver with such reference of designs with specific reference constant width and variable shift (b), specific reference variable width and shift (c), sun reference constant width and shift (d), sun reference constant width and variable shift (e) and sun reference variable width and shift (f), in June 21st.

In order to prove whether the new design implies an overall better performance or not, a ray tracing study is carried out. A validated program in Matlab [14] is used for this purpose, comparing first the radiation flux across the receiver and along one summer day in Almería, see Fig. 10[5]. The model uses Monte Carlo Ray Tracing algorithms, assuming the reflecting surface shape to cause Gaussian errors where $\sigma = 5$ mrad, and the solar disc intensity to follow the model given by Buie et al. [43], with a circumsolar factor of 5%.

Fig. 10a shows the flux intensity across the receiver along the day 21st June, for a solar field with the Fresdemo prototype design variables, assuming constant width and shift of mirrors with specific reference. In order to simplify the comparison between different designs, Fig. 10b–f depicts the difference in flux intensity between a given design and the constant width and shift with specific reference one, for each point of the receiver and for each time of the day, where the field width, the filling factor and the number of mirrors are maintained constant.

One may observe that the radiation flux in the receiver along the day is very similar no matter whether the innovative or the homogeneous configurations are used. Only variations of ± 1.5 kW/m^2 are observed, while the maximum radiation flux is around 70 kW/m^2. However, those differences show two clear tendencies:

- One may observe that a solar field where mirrors curvatures are given by a sun reference achieve higher radiation intensities at the center of the receiver than the same configuration with specific reference mirrors. This is due to the fact that off-axis aberration effects are minimized with such sun reference, as the maximum angle rotated by the mirrors from the reference position is lower. On the other hand, it seems that early in the morning and late in the afternoon the maximum differences deviate slightly from the receiver centerline. This is explained by the use of cylindrical mirrors instead of parabolic mirrors, which affect more importantly when the mirror is at one side of the contour parabola than when it coincides with the vertex of such parabola.
- When comparing different layouts of the mirrors it seems that the innovative solutions achieve higher radiation intensities at the center of the receiver. Nevertheless, this difference is not as high as when different mirror curvatures are compared, and they do not show the same trend at every time: early in the morning and late in the afternoon (when shading effects are predominant) the homogeneous distribution achieve higher intensities at the center of the receiver. This is due to the fact that the variable shift layouts have slightly higher shading effects in order to minimize and equilibrate blocking processes. However, at mid-morning and mid-afternoon, when the radiation becomes more important, this effect is reversed thanks to the fact that shading effects disappear while blocking effects become more important in the constant shift configuration. At midday blocking effects are also negligible, and thus differences in radiation between possible layouts of mirrors disappear.

Small radiation flux differences observed in Fig. 10 do not allow to ensure which technology, constant or variable widths and shifts, would achieve a better performance. For this reason, the energy efficiency along the year has been calculated for both systems via Monte Carlo Ray Tracing method. This simulation is carried out during 12 days of the year, weighting each simulation with a clearness factor from Refs. [51], taking points every 10 min when the DNI is higher than 600 W/m^2. The number of beams traced in each simulation is around 300,000.

Even though the simulation intends to analyze the optical performance of the field, the thermal process in the receiver cannot be obviated. High radiation intensities are necessary in order to drive a steam turbine. It is assumed that the HTF flows first within the

[5] The change in the location of the mirrors would drive to strong changes in the flux intensity at a given time from one configuration to the other due to the shadow projected by the receiver; in order to eliminate these differences, which do not affect the variation in the efficiency along the year, receiver shading has not been considered in simulations for a given day – Fig. 10 – although it has been considered for year simulations – Table 1.

outer tubes, where it heats up to an intermediate temperature, and then within the central tubes, where it achieves the final temperature [14]. Thus, the only requirement of the receiver to work is to be impinged at its central tubes with a radiation intensity above a given threshold that permits to achieve a given temperature.

In addition, it was proven in Ref. [16] that a radiation intensity of 25 kW/m^2 implies that the HTF can heat up to 400 °C with a good performance if the adequate selective coating is used. Therefore, the energy impinging onto the whole receiver at any instant will only be taken into account in the efficiency if the radiation intensity is above 25 kW/m^2 at the central part of the receiver. This would imply all radiation included in Fig. 10, which is a simulation during a summer day, but not around winter after simulations shown in Ref. [17]. On the other hand, impinging energy with radiation intensities bellow 5 kW/m^2 is not considered, as it would not be enough to heat the HTF above 300 °C [16].

The impinging energy with radiation intensity above 5 kW/m^2 when the radiation intensity at the central part of the receiver is above 25 kW/m^2 is called useful energy. Such value is compared with the energy that would impinge onto the mirrors if they were perpendicular to the impinging radiation at any time, with neither shading nor blocking effects and with two-axes tracking. That is to say, the divisor of the efficiency is the width of all mirrors (the width of the solar field times the filling factor) multiplied by the energy that would impinge onto one square meter receiver with two-axes tracking. With such definition, the energy efficiency gives an idea of the usefulness of the reflecting surface installed.

Results for all configurations and reference positions are given in Table 1.

The advantage of using sun reference versus specific reference is clearly observed in such results. A mean increase of 0.6 percentage points is obtained, which implies an increase in energy collected of 1.2% for the same mirrors surface. Therefore, from this study it is advised to give mirrors a curvature so that the mirror is focused when the sun is at its weighted typical position, i.e. the sun culmination at noon for NS embodiments.

On the other hand, the configuration of the field layout, for the Fresdemo design variables, does not have such a deep impact on the efficiency. It seems that the maximum efficiency is obtained with constant width and variable shift across the field, achieving an increase of around 0.2 percentage points compared to the homogeneous design. However, the design with variable width and shift of mirrors across the field seems to achieve an efficiency slightly lower than the constant width and variable shift, but higher than the homogeneous design.

The reasons why there is not a net efficiency improvement with variable width of mirrors compared to constant widths and variable shifts, although errors due to beam spread and to lateral drift are made equivalent, may be found in the fact that wide mirrors in the center of the field imply larger losses due to shading. Fig. 9 shows that the specific reference variable shift and width design, where the differences between narrow and wide mirrors are the largest, gets the maximum value of $\overline{f}_{t_e}$. This may explain why the efficiency is lower than in the case of constant width and variable shift between mirrors.

Table 1
Annual efficiency (%) of a NS solar field with Fresdemo design variables located in Almería, for constant and variable widths and/or shifts of mirrors, for specific and sun references.

	Specific reference	Sun reference
Cst. W & Cst. S	50.3%	50.9%
Cst. W & Var. S	50.5%	51.1%
Var. W & Var. S	50.5%	51.0%

Nevertheless, these results have been obtained for design variables of Fresdemo, which is a solar field designed for constant widths and shifts. An optimization of the field with the alternatives layouts must be carried out in order to obtain clear conclusions. In addition, this analytical design may be more interesting for EW embodiments, where $\overline{f}_{t_e}$ varies importantly across the field with homogeneous design.

5. Conclusions: a coherent design to improve the efficiency in radiation collection

An analytical study of the radiation concentration process in a linear Fresnel collector can help to improve the efficiency of the system. It has been seen that there are different reasons that drive to errors in the direction of the reflected beam, with a different effect depending on the width and location of the mirror. In addition, shading and blocking effects between neighboring mirrors depend as well on such variables. Therefore, the width and shift of mirrors may be varied across the field improving the efficiency of the system. Additionally, the curvature of mirrors must be studied, as it has a deep impact on the lateral drift of reflected rays along the day.

For the sake of an example, the Fresdemo design variables are used: 25 mirrors, relative field width of 2.625 and filling factor of 71.4%. It must be taken into account that such design variables have been chosen for a prototype with constant width and shift of mirrors across the field, and therefore it may occur that they are not perfectly suited for the innovative design.

When comparing solar fields where mirror curvatures are designed with specific or sun reference, it results that better performances are obtained with the latter. First, it is observed that higher radiation intensities are obtained in the center of the receiver, which may drive to a higher efficiency. This drives to an increase in the annual efficiency of around 0.6 percentage point, i.e. an increase in the power output of 1.2% for the same aperture area.

In addition, a solar field where the width of mirrors is constant, but the shift between them varies so that losses due to shading and blocking are equivalent across the field drive to an extra increase in the annual efficiency of 0.2 percentage point, i.e. increase of 0.4% in energy collected. However, the use of variable width mirrors does not seem to give a net efficiency increase compared to the variable shift and constant width design.

Such results must be regarded as a trend of efficiency improvements. Nevertheless, the design variables adopted for the study are not optimized neither for variable shift nor for variable width designs. Therefore, there is some future work projected now in optimizing the solar field for different number of mirrors, for constant and variables widths and shifts of mirrors. After such optimizations it will be possible to compare the optimum designs for each configuration, and thus conclude how far the efficiency can be improved.

Finally, this study should be carried out for East-West embodiments, where the effects of shading and blocking processes, as well as the off-axis aberration, vary sharply across the solar field.

Acknowledgments

Discussions with the rest of our Research Group are highly recognized.

Special thanks to "Fundación IBERDROLA", for their valuable support with the "Energía para la Investigación" program.

This research has been supported by the Ministerio de Economía y Competividad, project number "ENE2012-37950-C02-02".

References

[1] Haberle A, Zahler C, Lerchenmuller H, Mertins M, Wittwer C, Trieb F, et al. The Solarmundo line focussing Fresnel collector. Optical and thermal performance and cost calculations. In: 11th International SolarPACES Symposium on Solar Thermal Concentrating Technologies, Zurich, Switzerland; 2002.

[2] Nixon J, Dey P, Davies P. Which is the best solar thermal collection technology for electricity generation in north-west India? Evaluation of options using the analytical hierarchy process. Energy 2010;35(12):5230–40.

[3] Velázquez N, García-Valladares O, Sauceda D, Beltrán R. Numerical simulation of a linear Fresnel reflector concentrator used as direct generator in a solar-GAX cycle. Energy Convers Manag 2010;51(3). ISSN: 0196-8904:434–45.

[4] Singh P, Sarviya R, Bhagoria J. Heat loss study of trapezoidal cavity absorbers for linear solar concentrating collector. Energy Convers Manag 2010;51(2). ISSN: 0196-8904:329–37.

[5] Singh P, Sarviya R, Bhagoria J. Thermal performance of linear Fresnel reflecting solar concentrator with trapezoidal cavity absorbers. Appl Energy 2010;87(2). ISSN: 0306-2619:541–50.

[6] Gharbi N, Derbal H, Bouaichaoui S, Said N. A comparative study between parabolic trough collector and linear Fresnel reflector technologies. Energy Procedia 2011;6. ISSN: 1876-6102:565–72. impact of Integrated Clean Energy on the Future of the Mediterranean Environment?

[7] Facao J, Oliveira A. Numerical simulation of a trapezoidal cavity receiver for a linear Fresnel solar collector concentrator. Renew Energy 2011;36(1). ISSN: 0960-1481:90–6.

[8] Muñoz J, Martínez-Val J, Ramos A. Thermal regimes in solar-thermal linear collectors. Sol Energy 2011;85(5). ISSN: 0038-092X:857–70.

[9] Grena R, Tarquini P. Solar linear Fresnel collector using molten nitrates as heat transfer fluid. Energy 2011;36(2). ISSN: 0360-5442:1048–56.

[10] Pino F, Caro R, Rosa F, Guerra J. Experimental validation of an optical and thermal model of a linear Fresnel collector system. Appl Therm Eng 2011 ISSN: 1359-4311.

[11] Nixon J, Davies P. Cost-exergy optimisation of linear Fresnel reflectors. Sol Energy 2012;86(1). ISSN: 0038-092X:147–56.

[12] Morin G, Dersch J, Platzer W, Eck M, Haberle A. Comparison of linear Fresnel and parabolic trough collector power plants. Sol Energy 2012;86(1). ISSN: 0038-092X:1–12.

[13] Natarajan SK, Reddy K, Mallick TK. Heat loss characteristics of trapezoidal cavity receiver for solar linear concentrating system. Appl Energy. ISSN: 0306-2619.

[14] Abbas R, Montes M, Piera M, Martínez-Val J. Solar radiation concentration features in linear Fresnel reflector arrays. Energy Convers Manag 2012;54(1). ISSN: 0196-8904:133–44.

[15] Larsen SF, Altamirano M, Hernandez A. Heat loss of a trapezoidal cavity absorber for a linear Fresnel reflecting solar concentrator. Renew Energy 2012;39(1). ISSN: 0960-1481:198–206.

[16] Abbas R, Muñoz J, Martínez-Val J. Steady-state thermal analysis of an innovative receiver for linear Fresnel reflectors. Appl Energy 2012;92(0). ISSN: 0306-2619:503–15.

[17] Abbas R, Muñoz-Antón J, Valdés M, Martínez-Val J. High concentration linear Fresnel reflectors. Energy Convers Manag 2013;72(0). ISSN: 0196-8904:60–8.

[18] Sahoo SS, Varghese SM, Kumar CS, Viswanathan S, Singh S, Banerjee R. Experimental investigation and computational validation of heat losses from the cavity receiver used in linear Fresnel reflector solar thermal system. Renew Energy 2013;55(0). ISSN: 0960-1481:18–23.

[19] Manikumar R, Arasu AV. Heat loss characteristics study of a trapezoidal cavity absorber with and without plate for a linear Fresnel reflector solar concentrator system. Renew Energy 2014;63(0). ISSN: 0960-1481:98–108.

[20] N. R. E. Laboratory. Concentrating solar power projects. 2012. online, URL, http://www.nrel.gov/csp/solarpaces/.

[21] ProtermoSolar. Mapa de la Industria Solar Termoélectrica en España. 2012. online, URL, http://www.protermosolar.com/mapa.html.

[22] Häberle A, Zahler C, Lerchenmüller H, Mertins M, Wittwer C, Trieb F, et al. The Solarmundo line focussing Fresnel collector. Optical and thermal performance and cost calculations. In: Proceedings of the 2002 SolarPACES International Symposium; 2002.

[23] Mathur S, Kandpal T, Negi B. Optical design and concentration characteristics of linear Fresnel reflector solar concentrators–I. Mirror elements of varying width. Energy Convers Manag 1991;31(3). ISSN: 0196-8904:205–19.

[24] Mathur S, Kandpal T, Negi B. Optical design and concentration characteristics of linear Fresnel reflector solar concentrators–II. Mirror elements of equal width. Energy Convers Manag 1991;31(3). ISSN: 0196-8904:221–32.

[25] Morin G, Platzer W, Eck M, Uhlig R, Haberle A, Berger M, et al. Road map towards the demonstration of a linear Fresnel collector using a single tube receiver. In: 13th International SolarPACES Symposium on Solar Thermal Concentrating Technologies, Las Vegas, USA; 20–23, 2006.

[26] Bernhard R, Laabs H, De LaLaing J, Eck M, Eickhoff M, Pottler K, et al. Linear Fresnel collector demonstration on the PSA, part I–design, construction and quality control. In: 14th International SolarPACES Symposium on Solar Thermal Concentrating Technologies, Las Vegas, USA; 2008.

[27] Bernhard R, Hein S, De LaLaing J, Eck M, Eickhoff M, Pfander M, et al. Linear Fresnel collector demonstration on the PSA, part II–commissioning and first performance tests. In: 14th International SolarPACES Symposium on Solar Thermal Concentrating Technologies, Las Vegas, USA; 2008.

[28] Lin M, Sumathy K, Dai Y, Wang R, Chen Y. Experimental and theoretical analysis on a linear Fresnel reflector solar collector prototype with V-shaped cavity receiver. Appl Therm Eng 2013;51(1–2). ISSN: 1359-4311:963–72.

[29] Novatec-Solar, Novatec-Solar. 2012. online, URL, http://www.novatecsolar.com/.

[30] Areva, Areva-Solar. 2012. online, URL, http://www.areva.com/EN/global-offer-725/concentrated-solar-power-renewable-energies-solutions.html.

[31] MAN, Solar Power Group. 2012. online, URL, http://www.solarpowergroup.com.

[32] Choudhury C, Sehgal H. A fresnel strip reflector-concentrator for tubular solar-energy collectors. Appl Energy 1986;23(2). ISSN: 0306-2619:143–54.

[33] Negi B, Kandpal T, Mathur S. Designs and performance characteristics of a linear fresnel reflector solar concentrator with a flat vertical absorber. Sol Wind Technol 1990;7(4). ISSN: 0741-983X:379–92.

[34] Singh P, Ganesan S, Yadav G. Technical note:: performance study of a linear Fresnel concentrating solar device. Renew Energy 1999;18(3):409–16.

[35] Goswami R, Negi B, Sehgal H, Sootha G. Optical designs and concentration characteristics of a linear Fresnel reflector solar concentrator with a triangular absorber. Sol Energy Mater 1990;21(2–3). ISSN: 0165-1633:237–51.

[36] Sootha G, Negi B. A comparative study of optical designs and solar flux concentrating characteristics of a linear fresnel reflector solar concentrator with tubular absorber. Sol Energy Mater Sol Cells 1994;32(2). ISSN: 0927-0248:169–86.

[37] Chaves J, Collares-Pereira M. Etendue-matched two-stage concentrators with multiple receivers. Sol Energy 2010;84(2). ISSN: 0038-092X:196–207.

[38] Chaves J, Collares-Pereira M. Primary concentrator with adjusted etendue combined with secondaries associated to multiple receivers and with convection reduction. US Patent App. 12/993,478. 2011.

[39] Mills D, Morrison G. Compact linear Fresnel reflector solar thermal powerplants. Sol Energy 2000;68(3). ISSN: 0038-092X:263–83.

[40] Martínez-Val J, Valdés M, Abánades A, Amengual R, Piera M, Montes M, et al. Solar radiation concentration system, with linear mirrors and receiver. patent number ES 2 345 427 B2, Spain. 2011.

[41] Duffie J, Beckman W. Solar engineering of thermal processes. 2nd ed. John Wiley And Sons; 1991, ISBN 0-471-51056-4.

[42] Buie D, Dey C, Bosi S. The effective size of the solar cone for solar concentrating systems. Sol Energy 2003;74(5):417–27.

[43] Buie D, Monger A, Dey C. Sunshape distributions for terrestrial solar simulations. Sol energy 2003;74(2):113–22.

[44] Buie D, Monger A. The effect of circumsolar radiation on a solar concentrating system. Sol energy 2004;76(1):181–5.

[45] Kreith F, Goswami D. Handbook of energy efficiency and renewable energy. Mechanical engineering series. CRC Press; 2007, ISBN 9780849317309.

[46] Bendt P, Rabl A, Gaul H, Reed K. Optical analysis and optimization of line focus solar collectors. Tech. Rep. Golden, CO: National Renewable Energy Laboratory (NREL); 1979.

[47] Biggs F, Vittitoe CN. Helios model for the optical behavior of reflecting solar concentrators. Tech. Rep. Albuquerque, NM (USA): Sandia Labs; 1979.

[48] Pettit R, Biggs F, Vittitoe C. Simplified calculational procedure for determining the amount of intercepted sunlight in an imaging solar concentrator. J Sol Energy Eng 1983;105(1):101–7.

[49] Liu B, Jordan R. The interrelationship and characteristic distribution of direct, diffuse and total solar radiation. Sol Energy 1960;4(3):1–19.

[50] Steven M, Unsworth M. Shade-ring corrections for pyranometer measurements of diffuse solar radiation from cloudless skies. Q J R Meteorol Soc 1980;106(450):865–72.

[51] SoDa. Solar energy services for professionals. 2014. URL, http://www.soda-is.com/eng/index.html.